古 脊 椎 动 物 学 报
VERTEBRATA PALASIATICA

DOI: 10.19615/j.cnki.1000-3118.171023

# A new species of *Saurichthys* from the Middle Triassic (Anisian) of southwestern China

WU Fei-Xiang[1] SUN Yuan-Lin[2*] FANG Geng-Yu[3]

(1 *Key Laboratory of Vertebrate Evolution and Human Origins of Chinese Academy of Sciences*, *Institute of Vertebrate Paleontology and Paleoanthropology*, *Chinese Academy of Sciences* Beijing 100044)
(2 *Key Laboratory of Orogenic Belts and Crustal Evolution*, *School of Earth and Space Sciences*, *Peking University* Beijing 100871 *Corresponding author: ylsun@pku.edu.cn)
(3 *School of Public Health*, *Peking University* Beijing 100191)

**Abstract** The saurichthyiform fishes were effective predators and hence the significant consumers in the aquatic ecosystems during the Early Mesozoic. They showed a notable diversification in the Anisian (Middle Triassic) Lagerstätten of southwestern China. In this contribution, we report a new species of *Saurichthys* from the Anisian of Yunnan, China, that displays some peculiar modifications of the axial skeleton and the longate body of the group. This new species, *Saurichthys spinosa* is a small-sized saurichthyid fish characterized by a very narrow interorbital region of the skull roof, an anteriorly expansive and ventrally arched cleithrum, proportionally large abdominal vertebrae lacking neural spines and alternately bearing laterally-stretching paraneural plates, few fin rays in the median fins, and two paralleling rows of needle-like flank scales with strong thorns. This fish has slimmed down the body by reducing the depth of the head and the epaxial part of the trunk. The elongate paraneural plates inserted in the horizontal septum and the rigid interlocking of the flank scales render the fish a very stiff body, which is compatible with the functional consequence of the obvious decrease of the body (vertebral) segments. This discovery reveals the variability of the axial skeleton and the hydrodynamic properties of the saurichthyiform fishes. These factors, together with the innovations in the locomotion and feeding habit, might have intrinsically effected the evolutionary burst of the eastern Tethyan saurichthyiform fishes during the Anisian, a marked signature of the rapid radiation stage of the biotic recovery after the end-Permian extinction.

**Keywords** Luoping, Yunnan, Middle Triassic, *Saurichthys*, axial skeleton, body shape

**Citation** Wu F X, Sun Y L, Fang G Y, in press. A new species of *Saurichthys* from the Middle Triassic (Anisian) of southwestern China. Vertebrata PalAsiatica, DOI: 10.19615/j.cnki.1000-3118.171023



Following the devastating end-Permian mass extinction, the Triassic marine ecosystem had undergone a rapid recovery and eventual re-establishment by the Middle Triassic as a stable and complex system, a process that rebuilt a high diversity of marine fishes (Chen and Benton, 2012; Benton et al., 2013; Scheyer et al., 2014). The saurichthyiform fishes,

国家自然科学基金(批准号：41472019, 41172001, 41372016)、中国科学院青年创新促进会(编号：2017103)和现代古生物学和地层学国家重点实验室(中国科学院南京地质古生物研究所) (编号：123109)资助。
收稿日期：2017-07-03

characterized by a pointed head and a long body with posteriorly set median fins, are one of the most iconic fish lineages during this period (Romano et al., 2012; Benton et al., 2013; Scheyer et al., 2014). Soon after the mass extinction, they radiated all over the globe, invading both marine and freshwater ecosystems, and became particularly speciose during the Triassic (Romano et al., 2012; Kogan et al., 2015; Maxwell et al., 2016). As specialized predators, they were an important component of these aquatic ecosystems and retained the role of high-level consumers in the marine realm until they went to extinction in the Middle Jurassic (Chen and Benton, 2012; Romano et al., 2012; Maxwell et al., 2016).

Recent discoveries of saurichthyiform fishes from the Anisian Lagerstätten in southwestern China have vastly improved the understanding of these fishes (Wu et al., 2009, 2011, 2013, 2015; Zhang et al., 2010). To date, there are up to seven morphologically and ecologically distinct species emerging in a rather short interval (late Anisian). They show a notable disparity in the body size (Hu et al., 2011; Wu et al., 2011; Benton et al., 2013; Liu et al., 2014), the fin shape (Wu et al., 2011), and the feeding apparatus (Wu et al., 2013), suggesting the innovations in the locomotory pattern and the dietary preference of the saurichthyiform fishes. Except for these 'superficial' changes, they also exhibit some variations of the bones inside the body, namely the axial skeleton, regarding the structure of the haemal elements (Wu et al., 2015). The saurichthyiform axial skeleton, unique in the duplication of the vertebral elements, serves as the most important structural unit that backups the body elongation in this group (Maxwell et al., 2013) and its morphological changes therefore should have affected the functional properties of these fishes (Tintori, 1990; Kogan et al., 2015). According to current knowledge, the axial skeleton varies within this group in the degree of the development of the dorsal and ventral extension of the vertebrae, the neural spines and haemal spines, or the prezygapophyses of the neural arches (summarized in Wu et al., 2015; Maxwell et al., 2016). It is notable that these variations are confined in the vertical septum of the body and there is no signal of vertebral change in other aspect even in the species that show some tendency of widening the body (Wu et al., 2011). Here we report a new species of *Saurichthys* from the Anisian Luoping biota of Yunnan that shows additional growth of the axial skeleton in the horizontal dimension as a compensation for the loss of the neural spines in the dorsal vertical septum, which represents a new vertebral model of this group.

With a characteristic elongate body plan, the saurichthyiform fishes are considered as typical 'pike-like predators' and might have conducted fast-start or ambush predation (Kogan et al., 2015). For this predation pattern, the stiffness of the axial skeleton (body) and the contour of the body (e.g. fineness ratio, defined as the ratio of total body length to maximum body depth) are key functional properties that influence the efficiency of the hunting (Romano et al., 2012; Kogan et al., 2015). In generalized saurichthyiforms, the stiffness can be achieved either in the exoskeleton by the interlocking of the scutes along the dorsal and ventral midlines of the body (Rieppel, 1985; Wu et al., 2009, 2011, 2015; Kogan et al., 2015) or occasionally in the endoskeleton (vertebral bones) by the extraordinarily long processes directed both anteriorly and posteriorly from the neural arches (Tintori, 1990, 2013). The fineness ratio is a good indicator for the flow disturbance, pressure distribution and drag coefficient during the predation, which

are crucial factors influencing the outcome of the hunting of the saurichthyiform fishes (Kogan et al., 2015). This ratio is variable within this group, but it barely exceeds 18 and is mostly below 15, e.g. it is 12 in *Saurichthys curionii*, the model used in hydrodynamic analyses (Kogan et al., 2015). Here, the new species of *Saurichthys* has a very slim body with a fineness ratio of up to 20. On the basis of a detailed description of this new species, we highlight the peculiar modifications of the axial skeleton, the arrangement of the scale covering, as well as the changes of the body shape and their contributions to the stiffness and the slimness of the body. This contribution suggests the variability of these functional properties of the saurichthyiform fishes, which might be one aspect of the basis underlying the evolutionary success of these fishes during the Anisian when the marine ecosystem was fully recovered.

## 1 Materials and methods

The studied materials belong to the Institute of Paleontology and Paleoanthropology, Chinese Academy of Sciences (IVPP) and the Geological Museum of Peking University (GMPKU) and include 15 well-preserved specimens. They are from the middle unit (strata of Luoping biota) of the Upper Member of the Middle Triassic Guanling Formation exposed in the vicinity of Dawazi Village, Luoping County, Yunnan Province of China, and co-occur with several other saurichthyid species (Wu et al., 2009, 2011) (Fig. 1). Specimens were prepared using sharp needles. Line drawings were done based on photos, aided by constant

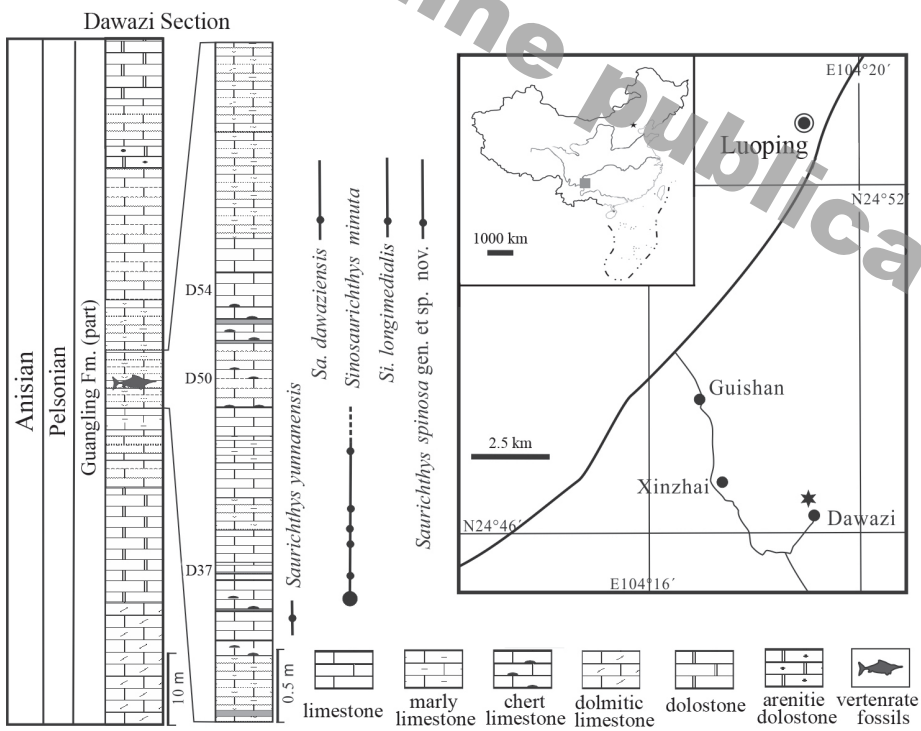


Fig. 1 Sketched location map and lithological column of the Middle Triassic Guanling Formation at Dawazi, Luoping County, Yunnan Province, China, with the stratigraphic distribution of some saurichthyid taxa
Modified from Wu et al., 2011

examination of the specimens under a Nikon SMZ1500 binocular. Neural arch numbers and maximum-recorded length were collected from published scientific literatures or personal observations. The sampled species are the ones known by complete materials. Scatter plot was drawn by Excel 2013 and Adobe Photoshop CS6. The goodness of fit ($R^2$) and the result of the hypothesis test were obtained by SPSS21.0.

## 2 Systematic paleontology

**Saurichthyiformes Aldinger, 1937 (*sensu* Berg, 1940)**

**Saurichthyidae Owen, 1860 (*sensu* Stensiö, 1925)**

***Saurichthys* Agassiz, 1834**

***Saurichthys spinosa* sp. nov.**

(Figs. 2–6)

**Diagnosis** A small-sized *Saurichthys* species characterized by a dorsoventrally compressed head with shallow mandibles; mandibular sensory canals opening via few longitudinal pits; very narrow interorbital region of cranial roof; heavily sculptured dermal skull roof with sensory canals marked by distinct ridges; cleithrum with an expanded anteroventral process, an accessory lateral process, and an arched ventral margin; axial skeleton comprising less vertebrae [ca. 54 (i.e. 108 neural arches, compared to 150–220 known in most of other saurichthyids)]; neural arches lacking neural spines throughout vertebral column and alternately bearing a transversal paraneural plate in abdominal region; scale cover including two needle-like flank (mid-lateral and ventrolateral) scale rows on either side; pectoral fin deep-based; median fins round in distal margin and comprising few and sparsely-set fin rays; median fin rays un-jointed and un-branched; some axonosts supporting fin rays of median fins in a one-to-one relationship.

**Holotype** IVPP V 23062 (Fig. 2A), a complete skeleton.

**Other referred specimens** IVPP V 23063, 22832; GMPKU-P-1533–1545.

**Locality** Dawazi Village, Luoping County, Yunnan Province, China (Fig. 1).

**Horizon** Middle part of the Upper Member of the Guanling Formation at the type locality, within the conodont *Nicoraella kockeli* Zone, Pelsonian substage of Anisian, Middle Triassic (Zhang et al., 2009).

**Etymology** *spinosa*, referring to the peculiar spinous scale covering of the fish.

## 3 Description

**General morphology** *Saurichthys spinosa* sp. nov. is a small-sized saurichthyid fish (Fig. 2), with an acuminate snout and an elongate body covered with six longitudinal rows of spinous scales. It bears round and posteriorly arranged dorsal and anal fins and a slightly forked symmetrical caudal fin. The standard body length (SBL) ranges from 65 to 97 mm and the skull length occupies ca. 28%–29% of the SBL.

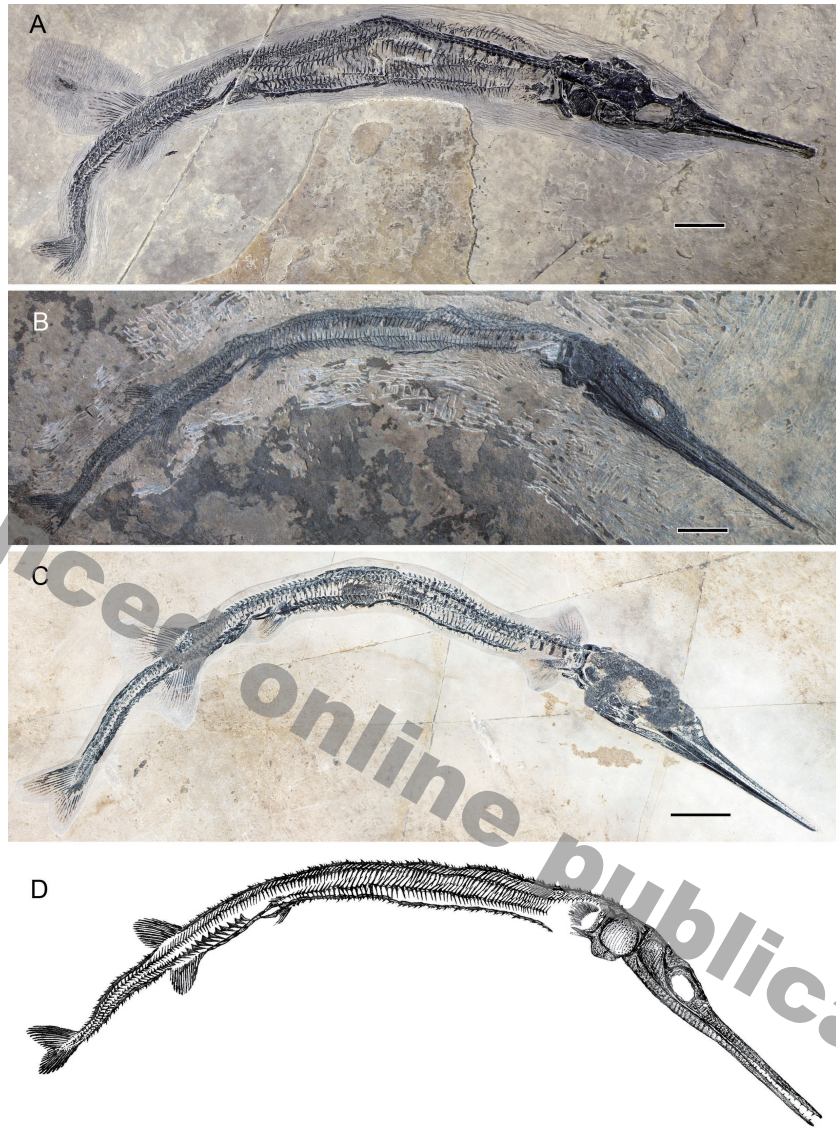




Fig. 2 Photographs (A–C) and tentative restoration (D) of *Saurichthys spinosa* sp. nov. A. IVPP V 23062 (holotype); B. GMPKU-P-1533; C. V 22832. Scale bars = 5 mm

**Neurocranium** The neurocranium, partially exposed in the orbit, is well ossified and delimits the posterior wall of the orbit (Figs. 3B, 4B). One or two openings are observed, which are possibly related to the cranial nerves or some vessels.

**Dermal skull roof** The skull roof is greatly constricted in the middle part of the frontals by the dorsal rims of the large orbits, such that the interorbital part of the cranial table is very narrow (Figs. 2A, 3, 4), and in the inner side this part is slightly hunched along the midline and there are no longitudinal ridges (Figs. 3B, 4B). Posteriorly, the skull roof is notably broadened. The parietals are represented by a heart-shaped region immediately behind the frontals, with no medial sutures clearly distinguishable. The paired dermopterotics meet along the midline,

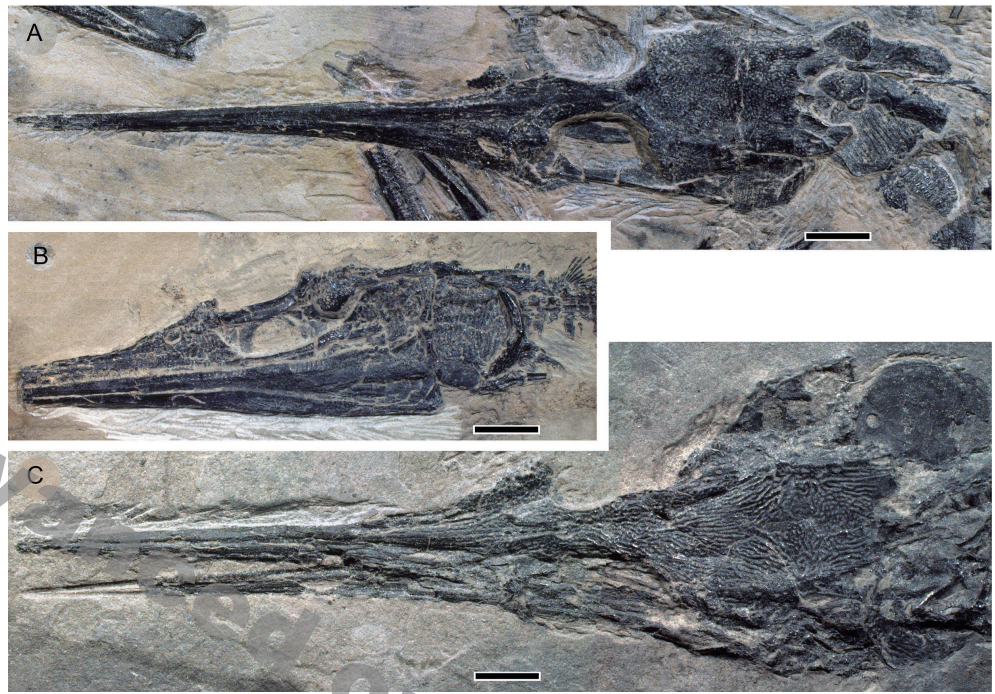


Fig. 3 Photographs of the skull of *Saurichthys spinosa* sp. nov.
A. GMPKU-P-1538; B. GMPKU-P-1536; C. GMPKU-P-1540. Scale bars = 2 mm

each has two embayments in the hind margin with the lateral one for the accommodation of the extrascapular (Figs. 3A, 4A) and the median one likely for the attachment of some soft tissues, respectively. The extrascapulars are cordiform in shape and each has a groove in the posterolateral part marking the temporal commissure of the sensory canals. The dermal cranial roof is heavily sculptured by irregular ridges and pits except that the extrascapulars bear some small tubercles on their surfaces (Figs. 3C, 4C), and the anterior portions of the frontals bear a series of thorns along the median suture between them.

The snout is long and acuminate (Figs. 2–4). The elongate rostro-premaxilla, fused with its antimere in the dorsal edge, tapers anteriorly to the tip and meets posteriorly with the maxilla below the anterior rim of the orbit. The triangular nasalo-antorbital wedges anteriorly between the frontal and the rostro-premaxilla and posteriorly makes up the anterior rim of the orbit. It bears two external nares on the outer surface, of which the anterior one is much larger than the posterior one. The supraorbital sensory canal passes between the nares and downward meets the sensory canals from the rostro-premaxilla and infraorbitals in a tri-radiate structure on the nasalo-antorbital (Fig. 4B). The lachrymal is small and oval in shape, bearing parts of the infraorbital canal. The rostro-premaxilla is covered with a few vertical stout ridges in the posterior part, and is smooth in the anterior portion. The nasalo-antorbital is ornamented with coarse tubercles and a few vertical strong ridges.

**Cheek region** The maxilla is slender in the suborbital part and is greatly expanded in the

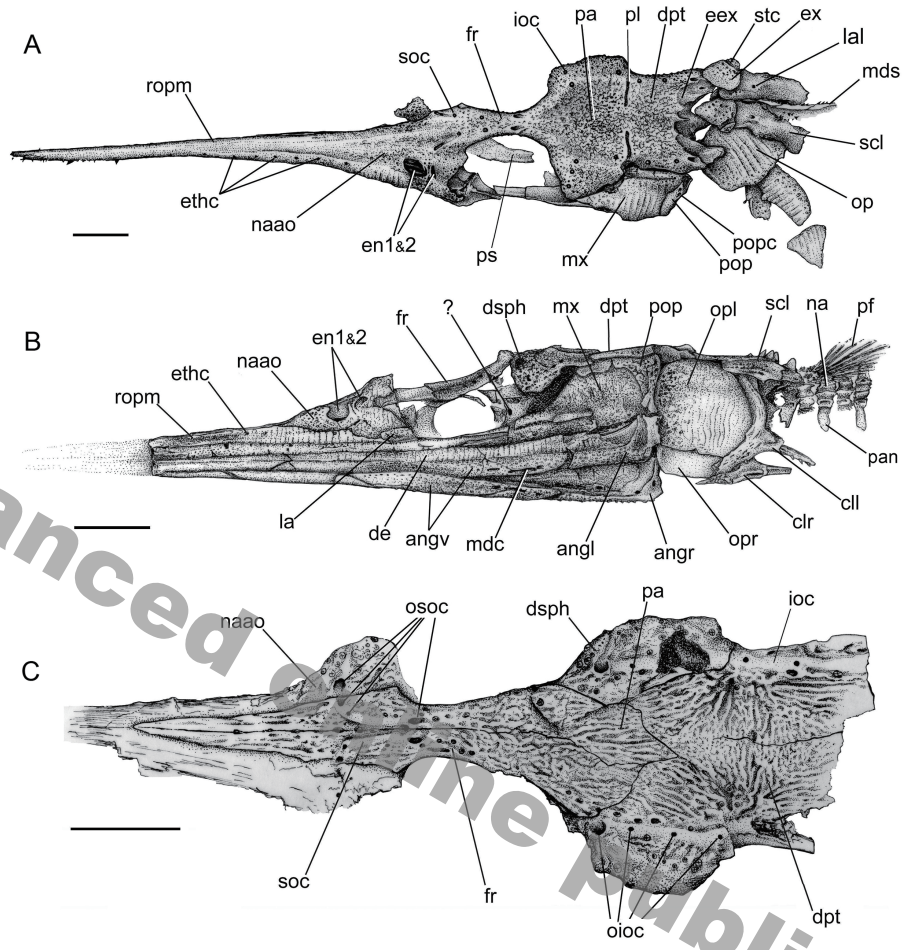


Fig. 4 Line drawings of the skull of *Saurichthys spinosa* sp. nov.
A. GMPKU-P-1538; B. GMPKU-P-1536; C. GMPKU-P-1540. Scale bars = 2 mm. Anterior facing left
Abbreviations: ?. an undetermined foramen on the neurocranium; angl, r. left and right angular; angv. ventral lamina of angular; cll, r. left and right cleithrum; de. dentary; dpt. dermopterotic; dsph. dermosphenotic; eex. embayment for receiving extrascapular; en1&2. anterior and posterior external nares; ethc. opening(s) of ethmoidal commissure (infraorbital canal); ex. extrascapular; fr. frontal; ioc. infraorbital sensory canal; la. lachrymal; lal. opening of lateral line; mdc. opening of mandibular sensory canal; mds. mid-dorsal scale row; mx. maxilla; na. neural arch; naao. nasaloantorbital; oioc. openings of infraorbital canal; op. opercle; opl, r. left and right opercle; osoc. openings of supraorbital sensory canal; pa. parietal; pan. alternating transversal paraneural plate; pf. pectoral fin; pl. pit line; pop. preopercle; popc. opening of preopercular sensory canal; ps. parasphenoid; ropm. rostropremaxilla; scl. supracleithrum; soc. supraorbital sensory canal; stc.supratemporal commissure of sensory canal

postorbital region. The preopercle is boomerang-like with the posterior edge slightly inclined posteriorly, making an acute angle in the posterodorsal corner (Fig. 4A, B) rather than a right or obtuse one in other known *Saurichthys* species and other saurichthyiforms (Stensiö, 1925; Lehman, 1952; Lehman et al., 1959; Griffith, 1962, 1977; Rieppel, 1980, 1985; Wu et al., 2009, 2011, 2013). The maxilla is mainly ornamented with stout and vertical ridges and some vermiculate rugae in the postorbital region, whereas the preopercle is much more weakly ornamented.

No circumorbital bones are observed in all available specimens, and their absence may not be preservational bias.

**Lower jaw** The mandible is shallow with the maximal depth slightly less than half of depth of the cheek region (measuring the height of the postorbital region of the maxilla plus the preopercle) (Figs. 3B, 4B). This is different from the mandible that is usually strong in the vast majority of saurichthyiform fishes with its maximal depth approximately equal to the cheek depth (Woodward, 1890; Stensiö, 1925; Piveteau, 1945; Gardiner, 1960; Griffith, 1959, 1962, 1977; Rieppel, 1980, 1985; Liu and Wei, 1988; Thies, 1985; Mutter et al., 2008; Kogan et al., 2009; Wu et al., 2009; 2011; 2013; 2015; Zhang et al., 2009; Maxwell et al., 2015; Kogan and Romano, 2016) but similar to the situation in three European Anisian species, *Saurichthys minimahleri* from Germany, *S. daubreei* from France and *S. dianneae* from the Netherlands, respectively (Werneburg et al., 2014; Maxwell et al., 2016). The mandible comprises a dentary, an angular and a supraangular on the lateral side and a prearticular, an articular, and at least two coronoids and partially the ventral flange of the angular on the median side. Of these bones, the articular, dentary, supraangular and prearticular are involved in forming the adductor fossa (Fig. 5A, B); however, it cannot be determined whether the coronoids also take part in that fossa or not.

The dentary occupies most of the lateral side of the mandible (Figs. 3B, 4B, 5A). It lacks ornamentation in the posteriormost and anterior third portions, and displays a few stout vertical ridges in the middle portion. Along the oral edge of the dentary, some large conical teeth are intervened with smaller ones. The angular is roughly triangular in shape and projects in its posteroventral corner, making a concave posterior edge of the lower jaw (Fig. 5A, B). It strongly flares inward along its ventral margin such that it produces a broad ventromedial flange toward the intermandibular region (Fig. 5B). This flange reaches its maximal width at the level of the middle portion of the mandible where it almost equals the maximal depth of the mandible (Fig. 5A, B). The supraanagular is slender and smooth. On the surface of the angular coarse and closely-set tubercles predominate.

In the medial view, the prearticular makes up most of the inner side of the mandible. It lacks any teeth in the posterior portion and bears numerous irregular depressions in the middle part (Fig. 5B). The coronoids are located along the dorsal edge of the prearticular (Fig. 5B). Based on the available materials, there are at least two coronoids, and both bear numerous tiny teeth that are much smaller than those on the dentary. There are three foramina in the posteroventral corner of the mandible. Among them, one lies on the suture between the angular and the prearticular and two on the angular, which are probably associated with the branches of the cranial nerves V and VII (Fig. 5B).

**Opercular apparatus** The opercle is roughly quadrate, slightly longer than deep (depth/length ratio ca. 0.93), with a slightly convex posterior edge [Figs. 3B, 4B, 5C (anterior edge incomplete)]. Its external surface is decorated with 18–20 stout vertical ridges and some irregular pits. Neither subopercle nor branchiostegal rays are discerned.

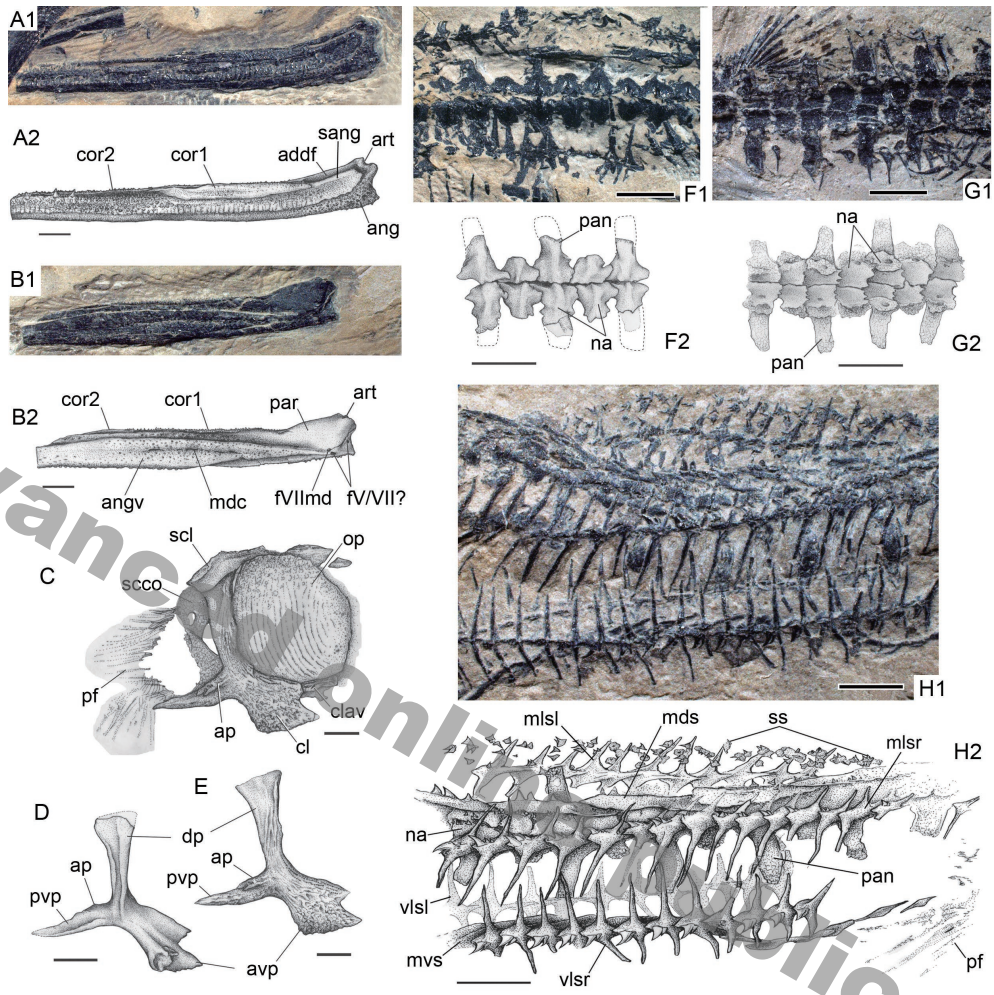


Fig. 5 Lower jaws, girdles and postcranial skeleton of *Saurichthys spinosa* sp. nov. A–B. left and right mandibles of GMPKU-P-1538 in lateral (A) and medial (B) views; C. right pectoral girdle and opercle of GMPKU-P-1533 (anterior edge of opercle broken) in lateral view; D. left cleithrum of GMPKU-P-1538 in median view; E. right cleithrum of GMPKU-P-1533 in lateral view; F–G. abdominal neural arches of GMPKU-P-1534 in dorsal view (F) and of GMPKU-P-1536 in ventral view (G); H. anterior abdominal region of GMPKU-P-1533 in lateral view. Anterior facing left in A, B, F, G and facing right in the rest. Dual figures with 1 and C–E for photographs, and 2 for line drawings. Scale bars = 1 mm

Abbreviations as in Fig. 4, plus: add.f. adductor fossa; ang. angular; ap. accessory process (posterolateral process) of cleithrum; art. articular; avp. anteroventral process of cleithrum; clav. clavical; cor1, 2. last and penultimate coronoids; dp. dorsal process of cleithrum; fV/VII?. foramina of ramus mandibularis trigemini or facialis; fVIImd. foramen of ramus mandibularis facialis; mlsl, r. left and right mid-lateral scale row; mvs. mid-ventral scale row; par. prearticular; pvp. posteroventral process; sang. supraangular; scco. scapulocoracoid; ss. tiny scattered spinous scales; vlsl, r. left and right ventrolateral scale row

**Sensory canals** The supraorbital and infraorbital sensory canals are arranged in a pattern similar to other saurichthyiforms (Stensiö, 1925; Lehman, 1952; Lehman et al., 1959; Rieppel, 1985; Wu et al., 2011, 2013, 2015; Romano et al., 2012). However, these sensory canals of the new species are distinct in the presence of prominent ridges marking their courses with large

but relatively few openings (4–5 for supraorbital canal and 6–7 for postorbital canal) on the skull roof (Fig. 4A, C). In some specimens, there are paired pit lines observed on the skull roof (Fig. 4A) that are comparable to the median branches of the infraorbital canals on the skull table in some Anisian *Saurichthys* species of Europe (Werneburg et al., 2014; Maxwell et al., 2016). The preopercular canal has several openings along the posterior edge of the preopercle. The mandibular canal opens outwards via a few short slot-like structures in the ventral flange of the angular (Figs. 4B, 5B), showing a condition different from other saurichthyiforms, in which a continuous series of pores extends throughout the lower jaw (Stensiö, 1925; Lehman, 1952; Gardiner, 1960; Rieppel, 1985; Wu et al., 2011, 2013, 2015; Maxwell et al., 2015).

**Axial skeleton** The axial skeleton consists of paired neural and haemal elements attached to the persisting notochord. There are ca. 108 (i.e. 54 vertebrae) neural arches anterior to the caudal fin, which represents much less vertebral elements than in the majority of the saurichthyiforms known to date (Rieppel, 1985, 1992; Wu et al., 2009, 2011, 2015; Maxwell et al., 2013, 2015; Kogan and Romano, 2016) but approximates that in two coeval species from the central Europe (Werneburg et al., 2014; Maxwell et al., 2016). The neural arches are relatively large and each roughly corresponds to one flank scale. The semi-neural arch meets its antimere along the midline (Fig. 5F, G). The prezygapophyses and postzygapophyses are very weakly developed. The neural arches lack neural spines throughout the vertebral column and bear a laterally extended plate in the base of every other abdominal arch (Figs. 3B, 4B, 5F, G, H, 6C). We name these plates as ‘paraneural plates’ following Arratia’s suggestions (personal communication, 2014). These plates are much longer than wide and gradually decrease in length posteriorly. The maximal length of these plates exceeds three times the width (in lateromedial dimension) of the neural arch. Among these plates, the longest one is at least three times the width of the associated neural arch. As the degree of the ossification decreases distally, the possibility cannot be ruled out that these plates might have been longer in living forms than those preserved in fossils. In medial view, a foramen is present in each plate-bearing neural arch.

The haemal elements are not clearly discernible except for the ones in the anterior caudal region. They display a one-to-one relationship to the neural arches and possess distinct haemal spines (Figs. 6A).

**Unpaired fins** The dorsal fin is rounded in the distal margin (Figs. 2, 6A). It comprises 22 sparsely arranged fin rays which are neither segmented nor bifurcated. Two radials (axonosts) can be observed; the first supports four rays and the second three rays.

The anal fin is slightly more posteriorly located than the dorsal fin (Figs. 2, 6A). It has 22 fin rays with an outline and arrangement of the rays similar to those of the dorsal fin. Six anterior radials (axonosts) are observed; among them, the first supports four fin rays, the second three rays, the third two fin rays, and the remaining three radials each holds a single fin ray. The posterior radials cannot be distinguished because of poor state of preservation.

The caudal fin is symmetrical with the body axis passing through between the epi- and

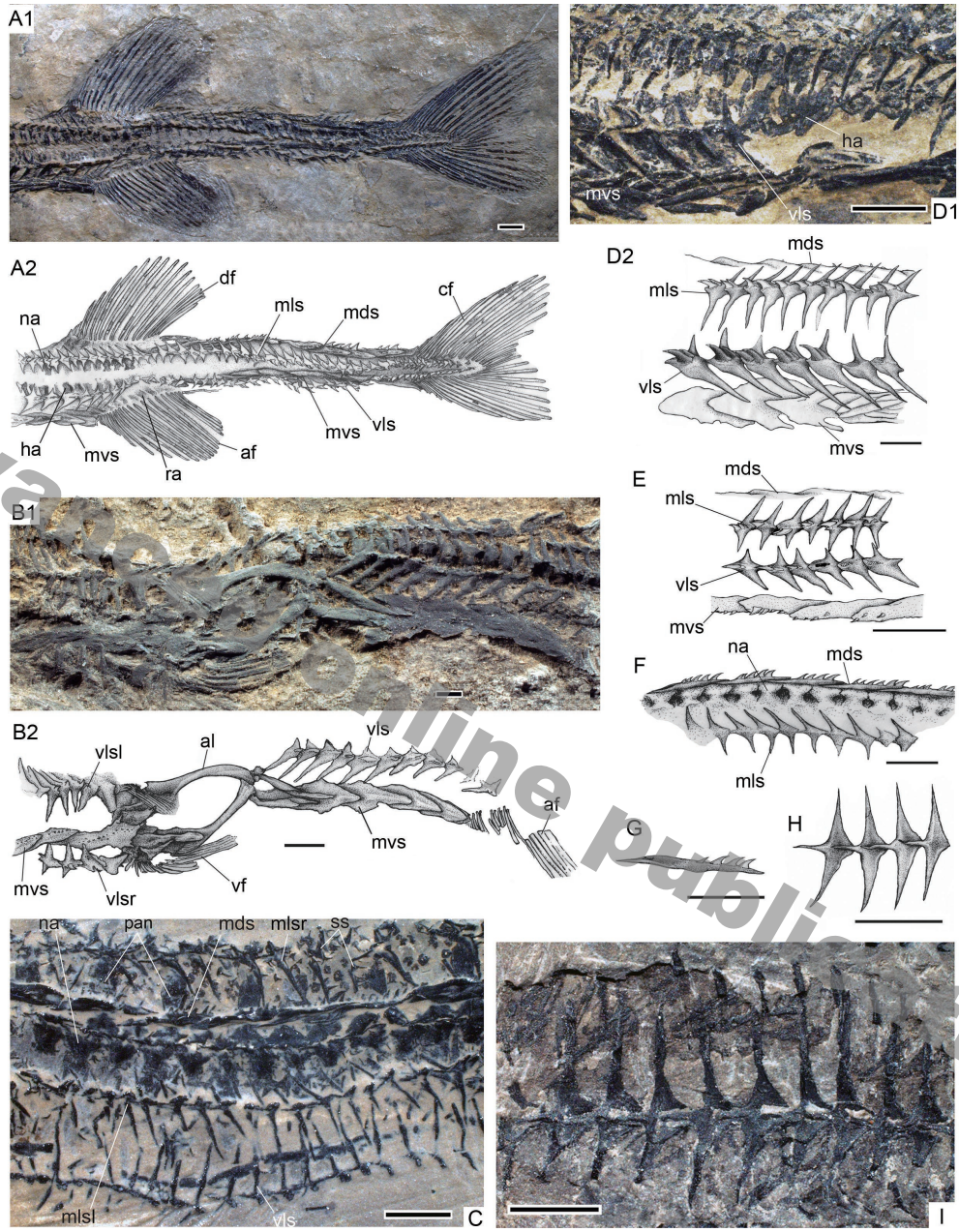


Fig. 6 Postcranial skeleton of *Saurichthys spinosa* sp. nov.

A. caudal region of GMPKU-P-1534; B. posterior abdominal region around pelvic fins in GMPKU-P-1542 showing the anal loop; C, F, G. GMPKU-P-1538: C. anterior abdominal region, F. dorsal aspect of mid-abdominal region, G. an isolated mid-dorsal scale in mid-abdominal region; D–E. GMPKU-P-1533: D. anterior caudal region, E. scales in anterior caudal peduncle; H–I. line drawing (H) and photograph (I) of abdominal right ventrolateral scale row of GMPKU-P-1541 in medial view. Scale bars = 1 mm. Anterior facing right in D, E and left in the rest. Dual figures with 1 and C, I for photographs, and 2 and E-H for line drawings Abbreviations as in Figs. 4, 5, plus: af. anal fin; al. anal loop; cf. caudal fin; df. dorsal fin; vf. pelvic fin; ha. haemal arch; mls. mid-lateral scale row; ra. radials; vls. ventrolateral scale row

hypochordal lobes (Figs. 2, 6A). The caudal fin is of a relatively low aspect ratio with both lobes being shallow and distally rounded. The caudal fork is not deep. The caudal fin rays are rigid and sparsely arranged, neither segmented nor bifurcated. Eighteen and nineteen fin rays are counted in the epichordal and hypochordal lobes, respectively, with the 11$^{th}$ ray being the longest in both lobes. The endoskeletal support of the caudal fin cannot be observed in current materials.

No fringing fulcra are developed on the leading edges of all median fins.

**Appendicular skeleton and paired fins** The dermal pectoral girdle consists of a supracleithrum, a cleithrum and a clavicle (Figs. 3A, B, 4A, B, 5C–E). No independent posttemporal is observed.

The supracleithrum (Figs. 4A, B, 5C) is roughly rectangular with a humped posterodorsal margin. The dorsal portion is smooth and the ventrolateral portion is decorated with some small serrated protuberances, indicating the facet covered by the opercle. Two pores of the lateral line are observed in the middle and posterolateral parts of the supracleithrum.

The cleithrum is generally triradiate in shape (Figs. 3B, 4B, 5C–E), consisting of a dorsal, a posteroventral, and an anteroventral process. The dorsal process increases in size dorsally until it articulates with the supracleithrum, the posteroventral process tapers distally, and the anteroventral process expands ventrally and articulate to the clavicle with a notched anterior margin (Fig. 5C–E). The anteroventral and posteroventral processes converge ventrally in such a way that they form an arcuate ventral margin of the cleithrum. Besides these three principal processes, there is also an accessory process emerging from the junction of the dorsal and posteroventral processes and bearing two or three spines at its tip (Fig. 5C, E). On the inner side of the cleithrum, a stout keel commences from the center of the bone and runs upwards along the anterior edge of the dorsal process. The ventral margin of the cleithrum is arched and thickened. The ornamentation on the outside surface consists of stout ridges radiating from the ossification center of the bone and some vermiculate ridges in the expanded portion of the anteroventral process. On the opercular facet enclosed by the anteroventral and the dorsal processes are some serrated ridges, as those on the comparable part of the supracleithrum referred above.

The exact shape of the clavicle cannot be determined. However, in GMPKU-P-1533, the clavicle is partially exposed and also shows some serrated structures similar to those on the comparable areas in other dermal pectoral girdle bones (Fig. 5C, E).

Of the endoskeletal girdle, the scapulocoracoid is well preserved in GMPKU-P-1533 (Fig. 5C). It is roughly rectangular, higher than wide, and anteriorly contacts the dorsal process of the cleithrum. There is two fenestrae in the scapulocoracoid; the anterior one is large and lies immediately posterior to the cleithrum and the posterior is smaller and posterodorsal to the anterior fenestra (Fig. 5C). The radials of the pectoral fins are not preserved. The pectoral fin consists of 12–13 unjointed fin rays and is deep-based, suggesting a nearly vertical insertion (Fig. 5C). No fringing fulcra are developed.

The pelvic fin is small and fan-like, comprising ca. 10 unjointed and unbranched fin rays

(Figs. 2, 6B). The pelvic girdle is not detectable. There are no fringing fulcra on the leading edge.

**Squamation** The new species bears six longitudinal scale rows on the trunk (a mid-dorsal, a mid-ventral, and paired mid-lateral and ventro-lateral scale rows), plus numerous scattered tiny spinous scales in the dorsal aspect of the body (Figs. 2, 5H, 6). The most notable features of the scale covering are the well-developed spines on the scales and the needle- or rib-like flank scales (the mid-lateral and ventro-lateral rows) (Figs. 2D, 5H, 6C–G).

The mid-dorsal scale row runs from the skull to the caudal fin, interrupted by the dorsal fin. There are 41 or 42 predorsal scales which are lanceolate in shape and gradually increase in size posteriorly. Each mid-dorsal scale consists of a V-shaped depressed anterior portion overlapped by the preceding scale and a posterior exposed portion carrying a longitudinal row of thorns (Figs. 5H, 6C–G). The scales in the caudal peduncle are similar to the predorsal ones in shape and structure, and slightly increase in size posteriorly towards the caudal fin. In total, 11 mid-dorsal scales are counted in the caudal peduncle.

The mid-ventral scale row begins from some distance behind the skull (Fig. 2B, D, 5H) and is branched at the level of the pelvic fins to form the anal loop (Fig. 6B). There are ca. 34 pre-pelvic scales. Of these scales, the one immediately in front of the anal loop is enlarged in the posterior part to contact that loop (Fig. 6B). The loop is composed of five scales of different shape and size on either branch. Of these loop scales, the first one is a small triangular scale and tapers posteriorly to superimpose upon the succeeding scale. The second one is broad in the anterior part but narrows posteriorly to articulate with the next one. The third one is the largest and like a ladle with a depressed anterior part and a gently laterally-bent body. Immediately next are two much smaller loop scales converging posteriorly towards the mid-ventral scale row anterior to the anal fin. Five lanciform mid-ventral scales are seen between the anal loop and anal fin and bear strong spines. The mid-ventral scales in the caudal peduncle mirror the morphology of the corresponding mid-dorsal scales (Fig. 6A). It is worthy of noticing that the spines on the abdominal mid-ventral scales are much more weakly developed (Fig. 2C) than those on the mid-dorsal scales in this region.

The mid-lateral scale row extends continuously throughout the trunk to the end of the body (Figs. 2, 5H, 6A, C–F). Just anterior to the caudal fin, the mid-lateral scales are triangular in shape. More anteriorly, they increase rapidly in size, and extend and taper both dorsally and ventrally, and hence possessing a needle- or rib-like appearance, especially for the ones in the abdominal region. When approaching the skull, they decrease in size again until attaching to the supracleithrum. These scales all bear strong and posteriorly directed spines in their central part. The spines are located in a row on the scale midline. The scales in the mid-abdominal region carry more spines (usually three spines per scale) than the scales elsewhere in the row. On the inner side, each abdominal scale bears an anteriorly tapering projection that underlies and extends until the anterior margin of the preceding scale, a structure also seen in the abdominal ventrolateral scales (Fig. 6H, I). This connecting pattern between neighboring

flank scales is not seen in any other known saurichthyiform fishes (Romano et al., 2012 and references therein), even those bearing similarly needle-like mid-lateral scales (Rieppel, 1985, 1992; Zhang et al., 2010; Werneburg et al., 2014; Maxwell et al., 2015, 2016). No openings for the lateral line canal can be detected on the mid-lateral scales.

The ventrolateral scale row begins behind the pectoral fin and is interrupted at the level of the pelvic fins and the anal loop (Figs. 2, 5H, 6A–E, H, I). These scales are generally similar in size but mirror the shape of the corresponding mid-lateral scales in the abdominal region and caudal peduncle. However, they are drastically enlarged in the length between the pelvic and the anal fins, such that one ventrolateral scale roughly spans two mid-lateral scales (Figs. 2, 6A, B, D). In medial view, all neighboring abdominal ventrolateral scales (except for the anteriormost one) show a similar articulation with that of the mid-lateral scales described above (Figs. 6H, I). On the central portion there are one or two posteriorly directed spines (occasionally three) on most abdominal scales. The ventrolateral and the mid-lateral scales are arranged in an interdigital pattern in the abdominal region, producing a unique flank scale covering never seen in most of the known saurichthyiform fishes to date (Woodward, 1890; Stensiö, 1925; Piveteau, 1945; Griffith, 1959, 1962, 1977; Gardiner, 1960; Rieppel, 1980, 1985; Thies, 1985; Liu and Wei, 1988; Mutter et al., 2008; Kogan et al., 2009, 2015; Wu et al., 2009, 2011; Romano et al., 2012; Kogan and Romano, 2016), including some *Saurichthys* species that have similar mid-lateral scales (Rieppel, 1985, 1992; Zhang et al., 2010; Maxwell et al., 2016). Interestingly, a similar arrangement of flank scales is seen in two species of *Saurichthys* from the Anisian of Germany and France (Werneburg et al., 2014), although the ventrolateral row is continuous in those species.

Besides the continuous scale rows, there are numerous tiny spinous scales confined in the region between the mid-dorsal and the mid-lateral scale rows (Figs. 5H, 6C). Each scale has a round base on which a spine emerges. This kind of spinous scales is not seen in the ventral aspect of the body.

## 4 Discussion

**Comparison** Many saurichthyid fishes were discovered from the Anisian of southwestern China (i.e. Panxian fauna in Guizhou and Luoping biota in Yunnan) (Wu et al., 2009, 2011, 2013, 2015; Zhang et al., 2009) and their nice preservation warrants a detailed comparison with the new species. *Saurichthys dawaziensis* is clearly distinguished from *S. spinosa* sp. nov. in having four rows of scales including the small, round mid-lateral scales and well-developed neural spines in the abdominal neural arches (Fig. 7A). *S. yangjuanensis* is much larger than the new species here and it has a totally different morphology of the flank scales, extensive segmentations of the lepidotrichia of the median fins and the axial skeleton with well-developed neural spines (Wu et al., 2015). *S. yunnanensis* resembles the new species in having rib-like mid-lateral scales; however, it is distinct from the new taxon in

having a much deeper lower jaw, a higher opercle and normally triangular ventrolateral scales in the abdominal region. In addition, *S. yunnanensis* has much more neural arches (at least 50 more than those in the new species) and much larger body size (Zhang et al., 2010). The *Sinosaurichthys* species differ from the new species here in having un-constricted interorbital region on the skull roof, a boot-like cleithrum, round mid-dorsal scales, much deeper opercles, triangular mid-lateral and roughly quadrate ventrolateral scales (Wu et al., 2011). They also differ from *S. spinosa* in the presence of much more neural arches surmounted with long neural spines and the absence of the paraneural plates in the abdominal section of the axial skeleton (Wu et al., 2011). Additionally, two species of the *Sinosaurichthys* show the peculiar elongation of the fins, which is not seen in the new species (Wu et al., 2011). *Yelangichthys macrocephalus* shows more notable differences in the very broad interorbital part of the skull table, the different arrangement of the parietal bones, the deep lower jaw, and other notable differences in the opercular shape and cleithral structure, as well as the small and screwdriver-like teeth (Wu et al., 2013).

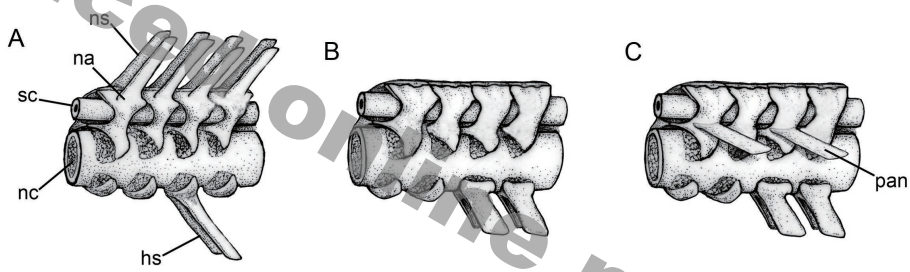


Fig. 7 Vertebral patterns in saurichthyiform fishes
A. neural arches with well-developed neural spines; B. neural arches lacking neural spines; C. neural arches lacking neural spines and carrying long paraneural plates (new species)
Anterior facing left and drawings not to scale
Abbreviations as to Fig. 4, plus: ns. neural spine; sc. spinal cord; nc. notochord; hs. haemal spine

The extensive constriction of the interorbital region in the skull roof is also recorded in some species from the Anisian of Europe, e.g., *Saurichthys daubreei*, *S. hoffmanni*, *S. minimahleri* and *S. dianneae* (Werneburg et al., 2014; Maxwell et al., 2016). They share with the new species the similar numbers of the neural arches, the lack of well-developed neural spines in the abdominal neural arches (Fig. 7B) and the rib-like mid-lateral scales; however, *S. daubreei* has a deeper opercle with the depth ratio of 0.7 (vs. 0.9 in new species) and the continuation of ventrolateral scales in the length spanning the pelvic fins and the anal loop (Werneburg et al., 2014: fig. 7), in contrast to the interruption of this scale row in *S. spinosa*. The materials of *S. hoffmanni* are very incomplete, inhibiting detailed comparison. But the acute embayment in the rear of the skull and the numerous and oblique striae on the lower jaw clearly distinguish it from the new species here. *S. minimahleri* is different from the new species in having the clearly quadripartite parietal complex, the continuous ventrolateral scales above the pelvic fins and anal loop, and a deeper opercle, and lacking the paraneural plates

in the abdominal neural arches (Werneburg et al., 2014). Meanwhile *S. dianneae* is divergent from *S. spinosa* in its tubercular ornamentation on the skull roof, a cleithrum with smaller dorsal and anterior processes, and the absence of the rib-like ventrolateral scales and the paraneural plates (Maxwell et al., 2016).

The needle-like mid-lateral scales are also developed in the *Saurichthys costasquamosus*, *S. paucitrichus*, *S. breviabdominalis* (i.e., species of the subgenus, *Costasaurichthys* proposed by Tintori, 2013, also see Maxwell et al., 2015); however, the structure of the axial skeleton in *S. spinosa* shows little resemblance to that of the *Costasaurichthys* species group, in which well-developed neural spines and much more numerous neural arches are present and the paraneural plates are absent. *Saurichthys striolatus* resembles the new species in the absence of the neural spines, but it differs from the latter taxon in lacking the paraneural plates. In addition, the two species are obviously different in the morphology of the scales. Moreover, *S. striolatus* has much more numerous neural arches (Griffith, 1959) than the new taxon.

**The modification of the body: a slim and stiffened body and possible functional implications** The new species has a typical saurichthyiform body shape, with the relative head length falling in the range of the majority of the saurichthyiform fishes known by complete specimens. However, it has modified this basic profile via reducing the depth of body in both dorsal and ventral parts. The change of the abdomen can be reflected by the change of the skull depth, as the latter roughly equals to the maximal body depth in saurichthyiform fishes. A much shallower lower jaw of the new species than in other saurichthyiforms leads to the reduction of the hypaxial depth of the trunk (Fig. 8A1, B1). From the dorsal side, the relevant feature is associated with the variation of the backbone. The vast majority of other saurichthyiform fishes usually bears well-developed neural spines in the abdominal vertebrae (Figs. 7A, 8A2); in sharp contrast, the new species completely lacks this part (Figs. 7C, 8B2), a specialization shared with few coeval species from the Middle Triassic of Europe (Werneburg et al., 2014) (Fig. 7B). The loss of the dorsal extensions (neural spines) of the axial skeleton and consequently the close proximity of the vertebral column to the dorsal ridge (mid-dorsal scales) (Fig. 6F) means that the axial column was embedded very close to the body surface and the epaxial part of the body was mostly squeezed out (Fig. 8B2). These modifications cause a very slim body with a fineness ratio of ca. 20, which is much higher than that in other contemporaries in China [*Saurichthys dawaziensis*, 17; *Sa. yunnanensis*, 12.7; *Sa. yangjuanensis*, ca. 15; *Sinosaurichthys longipectoralis*, 16, *Si. longimedialis*, average 16; *Si. minuta*, average 13; *Sinosaurichthys* sp., average 13 (IVPP V 23547 and V 23548)] and other saurichthyids elsewhere all over the world (Maxwell et al., 2015: fig. 9b). The body with such a high fineness ratio may be confronted with less drag and cause less flow disturbance during swimming, which are significant advantages for the predation (Kogan et al., 2015). To make use of these advantages, the fish has to maintain a steady body to minimize the undulation of the body during the crucial phrase of the attack (Kogan et al., 2015). In particular, for the slim new *Saurichthys* here, one solution is to increase the stiffness of the body.

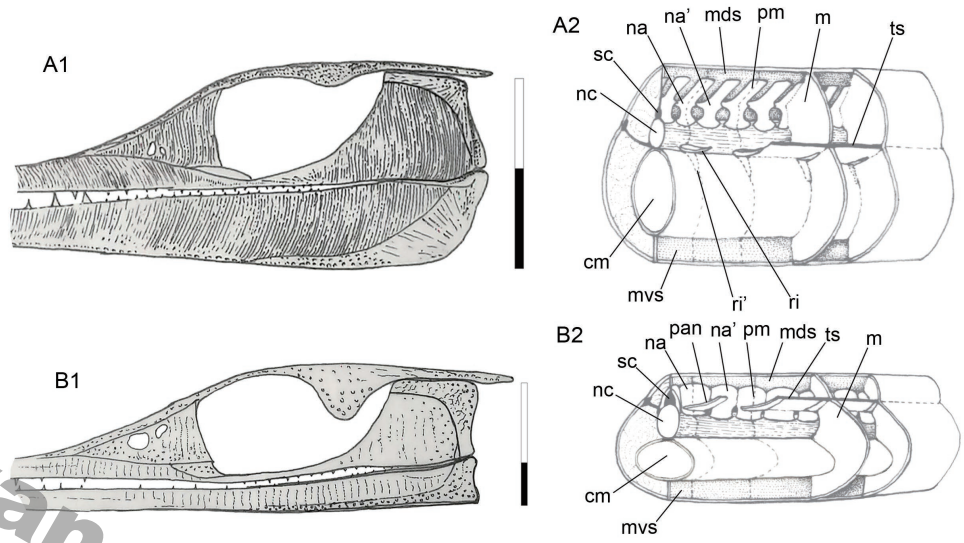


Fig. 8 Tentative restorations of the skull and simplified anatomical model of the anterior trunk to show the variations of the body shape and relevant structures within saurichthyiform fishes

A. generalized saurichthyiform fishes: A1. skull with a massive lower jaw, A2. anterior trunk with well-developed neural spines and large epaxial depth; B. *Saurichthys spinosa* sp. nov.; B1. skull with a shallow mandible, B2. anterior trunk with reduced epaxial and hypaxial depth. Bars in A1 and B1 showing the subdivision of the skull depth, with the white area being the depth of cheek region and the black one the maximal depth of lower jaw. Anterior facing left, figures not to scale

Abbreviations as to Figs. 4, 7, plus: cm. coelom; m. vertical septum; mds. mid-dorsal septum; mvs. mid-ventral septum; na'. second neural arch in one vertebral unit; pm. presumed position of vertical transverse septum; ri. rib-like structure; ri'. alternative position of the rib-like structure; ts. transverse or horizontal septum

The vertebral counts (neural arches) of the new species are among the minimal record in known saurichthyiforms (see Maxwell et al., 2015, 2016; Wu et al., 2015) except for few coeval *Saurichthys* species from Europe (Werneburg et al., 2014; Maxwell et al., 2016), which indicates that the new fish has much less body segments than the vast majority of saurichthyiform fishes (see Maxwell et al., 2015, 2016; Wu et al., 2015; Fig. 9), e.g. approximating only half that of its contemporary, *Sinosaurichthys longipectoralis* from the adjacent and coeval Panxian fauna in Guizhou Province (Wu et al., 2011). This is reminiscent of Lindsey's (1975) 'Pleomersim', a phenomenon of the vertebral number being positively correlative to the maximal body length in fishes, as the new species is among the smallest members of the saurichthyiform fishes (Maxwell et al., 2016). And indeed, the scatterplot diagram shows correlation between the body length and the vertebral number within this group (Fig. 9). And interestingly, if the sampling list excludes the *Sinosaurichthys* species, the correlation between these two parameters is more significant (Fig. 9). However, there are exceptions, e.g. the Late Triassic species *Saurichthys striolatus* with 180–190 neural arches in a body of ca. 10–18 cm long, but its exceptionally large skull/body length ratio (40%–45%, *vs*. less than 30% in the new species) implies that the measured specimens (Griffith, 1959)

may represent juvenile individuals according to the ontogenetic trajectory of the skull in saurichthyiform fishes (Bürgin, 1990; Rieppel, 1992). From the functional perspective, the quantitative reduction of the vertebrae makes sense for the new fish. The notable decrease of the body (vertebral) segments' amount in a given body plan will consequently reduces the lateral flexibility of the fish body (Lindsey, 1975). This is consistent with the functional consequence of the specializations of the axial skeleton and the flank scales. Judging from the general arrangement of the myotomes and the septa in fishes (Goodrich, 1930), the wide and horizontally-set paraneural plates (Fig. 7C) must be inserted in and hence being tightly fixed by the horizontal septum (Fig. 8B2). In this way, these plates would have minimized the lateral displacement of the backbone and thereby stiffened the axial skeleton and eventually, the fish body, probably as the epineural tendons do in living fishes (Gemballa and Treiber, 2003). In addition, the articulation pattern and the paralleling arrangement of the needle-like flank scales have also contributed to the stiffness of body. The peculiar interlock of the successive flank scales (e.g., mid-lateral scale row) (Fig. 6H, I) limits the lateral undulation of the body, an effect further strengthened by its duplication in another paralleling flank scale row (ventrolateral row) (Fig. 2). Given these peculiar modifications, some of which are unique herein, the new fish therefore might have a stiffer body than its saurichthyiform relatives known to date, and naturally has a greater potential to optimize the predation by minimizing the additional drag and the flow disturbance to avoid being detected by the prey (Kogan et al., 2015).

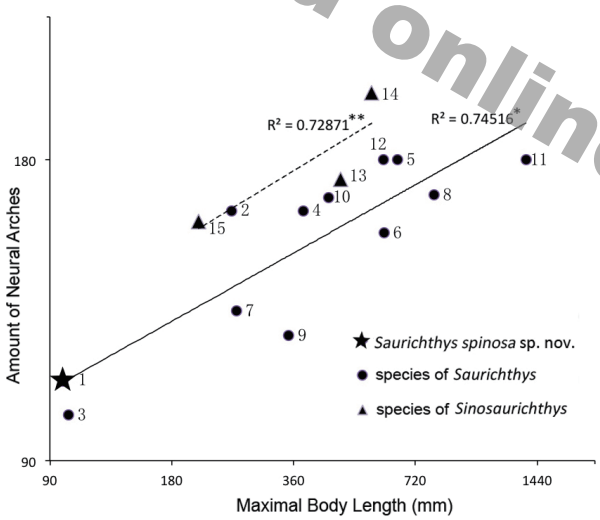


Fig. 9 Relation of mean neural arch number to maximum body length in saurichthyid fishes known as complete materials
The plot is presented in logarithmic axes. Each point represents a *Saurichthys* or *Sinosaurichthys* species. 1. *Saurichthys spinosa* sp. nov.; 2. *S. microcephalus*; 3. *S. minimahleri*; 4. *S. dawaziensis*; 5. *S. yangjuanensis*; 6. *S. rieppeli*; 7. *S. paucitrichus*; 8. *S. costasquamosus*; 9. *S. breviabdominalis*; 10. *S. curionii*; 11. *S. grignae*; 12. *S. madagascariensis*; 13. *Sinosaurichthys longimedialis*; 14. *Si. longipectoralis.* 15. *Si. minuta.* * $P < 0.001$; ** $P > 0.05$. The broken line represents the relation in *Sinosaurichthys* and the black line represents that in *Saurichthys*

The saurichthyiform fishes were abundant and diverse, both morphologically and taxonomically, in the Middle Triassic faunas of southwestern China. *Saurichthys spinosa* sp. nov. here is the ninth species of this group in this region during the late Anisian of the early Middle Triassic (Wu et al., 2009, 2011, 2013, 2015; Zhang et al., 2010). And the undescribed materials and ongoing field explorations promise more findings ahead. It is a lightspot of the evolutionary history of the marine fishes during this crucial stage

of the biotic recovery, as no other contemporary fish group known to date has diversified in such a magnitude (Xu and Wu, 2012; Xu et al., 2012, 2014, 2015; Benton et al., 2013; Tintori, 2013; Tintori et al., 2014). The new species expands the spectrum of the body size of this group in eastern Tethys and suggests the considerable disparity of the axial skeletal, the scale covering, and some relevant functional properties of the body in this group. This reflects the extraordinary plasticity of the saurichthyiform fishes, which may represent the intrinsic mechanism underlying their evolutionary burst during the radiation stage of the marine ecosystem after the end-Permian mass extinction (Chen and Benton, 2012; Benton et al., 2013).

**Acknowledgements** The authors thank MM Chang, GH Xu, G Arratia and I Kogan for helpful discussion. Thanks to ZY Sun, DY Jiang, WC Hao for their help in the fossil collection. Thanks to W Gao and GH Xu for photographing some fossil specimens (Fig. 2A, B) and J Zhong for preparing the holotype (Fig. 2A, C); Thanks also to M Richter and Z Johanson for their help with the collection visit in British Museum of Natural History, and H Furrer, E Maxwell and JD Carrillo-Briceño in Paläontologisches Institut und Museum, Universität Zürich and LJ Zhao in Zhejiang Museum of Natural History, QY Zhang, SX Hu and W Wen in Chengdu Institute of Geology and Mineral Resources. Many thanks to the reviewers, I Kogan and GH Xu, for their valuable suggestions. Special thanks are due to the editorial production team. This work was supported by the National Natural Science Foundation of China (grant nos. 41472019, 41172001, 41372016), Youth Innovation Promotion Association, CAS (2017103) to FX Wu, the State Key Laboratory of Palaeobiology and Stratigraphy (NIGP, CAS) (grant no. 123109).



## 我国西南地区中三叠世安尼期龙鱼属(*Saurichthys*)一新种

吴飞翔[1] 孙元林[2] 房庚雨[3]

(1 中国科学院古脊椎动物与古人类研究所，中国科学院脊椎动物演化与人类起源重点实验室 北京 100044)

(2 北京大学地球与空间科学学院，造山带与地壳演化重点实验室 北京 100871)

(3 北京大学公共卫生学院 北京 100191)

**摘要**：作为一类高效的捕食者，龙鱼跻身中生代早期水生生态系统中的重要消费者。我国西南地区中三叠世安尼期的化石群中，龙鱼类在形态和分类上呈现出显著的多样性。报道了云南安尼期罗平生物群的龙鱼属(*Saurichthys*)一新种，它代表着龙鱼在椎骨结构和基本体型上的新变化。披刺龙鱼(新种) (*Saurichthys spinosa* sp. nov.)是一种小型龙鱼，其特征包括：颅顶部的眶间区(interorbital region)非常狭窄；匙骨前端膨大而腹侧呈拱状；椎骨偏大且无神经棘，侧向伸展的副神经板(paraneural plate)在躯椎里交替出现；奇鳍鳍条数量较少；体表具两列平行的披强壮棘刺的针状侧鳞。与同属其他种类相比，*S. spinosa*头部及躯体轴上部的高度明显减缩以致体高变小。体内侧向延长并插入水平膈的副神经板与体表刚

性互锁的双排侧鳞使得整个鱼体非常僵硬，这与其体节(椎骨)数目的减少在功能上具有一致性。这一发现揭示了龙鱼类中轴骨骼结构及其体型流体力学特质的多样化。综合同时期龙鱼类在运动方式和摄食机制的创新，这些因素可能促成了安尼期东特提斯洋龙鱼类的爆发式演化，而这正是二叠纪末大绝灭后生物圈复苏过程中快速辐射阶段的一个缩影。

**关键词：**云南罗平，中三叠世，龙鱼属 (*Saurichthys*), 中轴骨骼，体型

## References

Benton M J, Zhang Q Y, Hu S X et al., 2013. Exceptional vertebrate biotas from the Triassic of China, and the expansion of marine ecosystems after the Permo-Triassic mass extinction. Earth-Sci Rev, 125: 199–243

Bürgin T, 1990. Reproduction in Middle Triassic actinopterygians; complex fin structures and evidence of viviparity in fossil fishes. Zool J Linn Soc, 100: 379–391

Chen Z Q, Benton M J, 2012. Timing and pattern of biotic recovery following the end-Permian mass extinction. Nat Geosci, 5: 1–9

Gardiner B G, 1960. A review of certain actinopterygian and coelacanth fishes, chiefly from the Lower Lias. Bull Br Mus (Nat Hist), Geol, 4: 239–384

Gemballa S, Treiber K, 2003. Cruising specialists and accelerators – Are different types of fish locomotion driven by differently structured myosepta? Zoology, 106: 203–222

Goodrich E S, 1930. Studies on the Structure and Development of Vertebrates. London: Macmillan. 1–837

Griffith J, 1959. On the anatomy of two saurichthyid fishes, *Saurichthys striolatus* (Bronn) and *S. curionii* (Bellotii). Proc Zool Soc London, 132: 587–606

Griffith J, 1962. The Triassic fish *Saurichthys krambergeri* Schlosser. Palaeontology, 5: 344–354

Griffith J, 1977. The Upper Triassic fishes from Polzberg bei Lunz, Austria. Zool J Linn Soc, 60: 1–93

Hu S X, Zhang Q Y, Chen Z Q et al., 2011. The Luoping biota: exceptional preservation, and new evidence on the Triassic recovery from end-Permian mass extinction. Proc R Soc B, 278: 2274–2282

Kogan I, Romano C, 2016. Redescription of *Saurichthys madagascariensis* Piveteau, 1945 (Actinopterygii, Early Triassic), with implications for the early saurichthyid morphotype. J Vert Paleont, 36: 4, e1151886

Kogan I, Schönberger K, Fischer J et al., 2009. A nearly complete skeleton of *Saurichthys orientalis* (Pisces, Actinopterygii) from the Madygen Formation (Middle to Late Triassic, Kyrgyzstan, central Asia) – preliminary results. Freiberg Forschungs C532, 17: 139–152

Kogan I, Pacholak S, Licht M et al., 2015. The invisible fish: hydrodynamic constraints for predator-prey interaction in fossil fish *Saurichthys* compared to recent actinopterygians. Biol Open, 4: 1715–1726

Lehman J P, 1952. Etude complémentaire des poissons de l'Eotrias de Madagascar. K Svenska VetAkad Handl, Ser 4, 2(6): 1−201

Lehman J P, Chateau C, Laurian M et al., 1959. Paléontologie de Madagascar, XXVIII. Les poisons de la Sakamena Moyenne. Ann Paléont, 45: 177−219

Lindsey C C, 1975. Pleomerism, the widespread tendency among related fish species for vertebral number to be correlated with maximum body length. J Fish Res Board Can, 32: 2453−2469

Liu J, Hu S X, Rieppel O et al., 2014. A gigantic nothosaur (Reptilia: Sauropterygia) from the Middle Triassic of SW China and its implication for the Triassic biotic recovery. Sci Rep, 4: 7142

Liu X T, Wei F, 1988. A new saurichthyid from the Upper Permian of Zhejiang, China. Vert PalAsiat, 26(2): 77–89

Maxwell E E, Furrer H, Sänchez-Villagra M R, 2013. Exceptional fossil preservation demonstrates a new mode of axial skeleton elongation in early ray-finned fishes. Nat Commun, 4: 2570, doi: 10.1038/ncomms3570

Maxwell E E, Romano C, Wu F X et al., 2015. Two new species of *Saurichthys* (Actinopterygii: Saurichthyidae) from the Middle Triassic of Monte San Giorgio, Switzerland, with implications for character evolution in the genus. Zool J Linn Soc, 173: 887–912

Maxwell E E, Diependaal H, Winkelhorst H et al., 2016. A new species of *Saurichthys* (Actinopterygii: Saurichthyidae) from the Middle Triassic of Winterswijk, The Netherlands. Neues Jahrb Geol Paläont, Abh, 280: 119–134

Mutter R J, Cartanyà J, Basaraba S A U, 2008. New evidence of *Saurichthys* from the Lower Triassic with an evaluation of early saurichthyid diversity. In: Arratia G, Schultze H P, Wilson M V H eds. Mesozoic Fishes 4 – Homology and Phylogeny, Proceedings of the International Meeting Miraflores de la Sierra, 2005. München: Verlag Dr. Friedrich Pfeil. 103–127

Piveteau J, 1945. Les poissons du Trias inférieur, la famille das Saurichthyidés. Paléontologie de Madagascar, XXV. Ann Paléont, 31: 79–87

Rieppel O, 1980. Additional specimens of *Saurichthys madagascariensis* Piveteau, from the Eotrias of Madagascar. Neues Jahrb Geol Paläont, Monatsh, 1980: 43–51

Rieppel O, 1985. Die Triasfauna der Tessiner Kalkalpen. XXV. Die Gattung *Saurichthys* (Pisces, Actinopterygii) aus der mittleren Trias des Monte San Giorgio, Kanton Tessin. Schweiz Paläont Abh, 108: 1–103

Rieppel O, 1992. A new species of the genus *Saurichthys* (Pisces: Actinopterygii) from the Middle Triassic of Monte San Giorgio (Switzerland), with comments on the phylogenetic interrelationships of the genus. Palaeontogr Abt A, 221: 63–94

Romano C, Kogan I, Jenks J et al., 2012. *Saurichthys* and other fossil fishes from the late Smithian (Early Triassic) of Bear Lake County (Idaho, USA), with a discussion of saurichthyid palaeogeography and evolution. Bull Geosci, 87: 543–570

Scheyer T M, Romano C, Jenks J et al., 2014. Early Triassic marine biotic recovery: the predators' perspective. PLoS ONE, 9(3): e88987

Stensiö E A, 1925. Triassic fishes from Spitzbergen, Part II. K Svenska VetAkad Handl, Ser 3, 2(1): 1–261

Thies D, 1985. Funde von *Acidorhynchus brevirostris* (Woodward 1895) aus dem Posidonienschiefer (Unter-Toarcium) NW-Deutschlands. Palaeontogr Abt A, 187: 183–203

Tintori A, 1990. The vertebral column of the Triassic fish *Saurichthys* (Actinopterygii) and its stratigraphical significance. Riv Ital Paleont Stratigr, 96: 93–102

Tintori A, 2013. A new species of *Saurichthys* (Actinopterygii) from the Middle Triassic (early Ladinian) of the northern Grigna Mountain (Lombardy, Italy). Riv Ital Paleont Stratigr, 119: 287–302

Tintori A, Hitij T, Jiang D Y et al., 2014. Triassic actinopterygian fishes: the recovery after the end-Permian crisis. Integr Zool, 9: 394–411

Werneburg R, Kogan I, Sell J, 2014. *Saurichthys* (Pisces: Actinopterygii) aus dem Buntsandstein des Germanischen Beckens. Semana, 29: 3–35

Woodward A S, 1890. The fossil fishes of the Hawkesbury series at Gosford. Mem Geol Surv New South Wales, 4: 1–55

Wu F X, Sun Y L, Hao W C et al., 2009. A new species of *Saurichthys* (Actinopterygii: Saurichthyidae) from Middle Triassic (Anisian) of Yunnan Province, China. Acta Geol Sin-Engl, 83: 440–450

Wu F X, Sun Y L, Xu G H et al., 2011. New saurichthyid actinopterygian fishes from the Anisian (Middle Triassic) of southwestern China. Acta Palaeont Pol, 56: 581–614

Wu F X, Chang M M, Sun Y L et al., 2013. A new saurichthyiform (Actinopterygii) with a crushing feeding mechanism from the Middle Triassic of Guizhou (China). PloS ONE, 8: e81010

Wu F X, Sun Y L, Hao W C et al., 2015. A new species of *Saurichthys* (Actinopterygii; Saurichthyiformes) from the Middle Triassic of southwestern China, with remarks on pattern of the axial skeleton of saurichthyid fishes. Neues Jahrb Geol Paläont, Abh, 275: 249−267

Xu G H, Shen C C, 2015. *Panxianichthys imparilis* gen. et sp. nov., a new ionoscopiform (Halecomorphi) from the Middle Triassic of Guizhou, China. Vert PalAsiat, 53(1): 1–15

Xu G H, Wu F X, 2012. A deep-bodied ginglymodian fish from the Middle Triassic of eastern Yunnan Province, China, and the phylogeny of lower neopterygians. Chin Sci Bull, 57: 111−118

Xu G H, Zhao L J, Gao K Q et al., 2012. A new stem-neopterygian fish from the Middle Triassic of China shows the earliest over-water gliding strategy of the vertebrates. Proc R Soc B, 280: 20122261

Xu G H, Shen C C, Zhao L J, 2014. *Pteronisculus nielseni* sp. nov., a new stem-actinopteran fish from the Middle Triassic of Luoping, Yunnan Province, China. Vert PalAsiat, 52(4): 364−380

Zhang Q Y, Zhou C Y, Lü T et al., 2009. A conodont-based Middle Triassic age assignment for the Luoping biota of Yunnan, China. Sci China Ser D: Earth Sci, 52: 1673–1678

Zhang Q Y, Zhou C Y, Lü T et al., 2010. Discovery of Middle Triassic *Saurichthys* in the Luoping area, Yunnan, China. Geol Bull China, 29: 26–30